APPLICATIONS OF
MODELLING AND SIMULATION
http://arqiipubl.com/ams eISSN 2600-8084 VOL 4, 2020, 149-158

Parametric Study of Polypropylene Based Geotextile Mat for Optimum Performance in Engineered Landfill Systems

Aniekan Essienubong Ikpe[1], Ndon Akanu-ibiam Effiong[2] and Etuk Ekom Mike[3]

[1]Department of Mechanical Engineering, University of Benin, P.M.B. 1154, Nigeria
[2]Department of Civil Engineering, Akwa Ibom State University, Mkpat Enin, Akwa Ibom State, Nigeria
[3]Department of Production Engineering, University of Benin, P.M.B. 1154, Benin, Edo State, Nigeria

*Corresponding author: aniekan.ikpe@eng.uniben.edu

Submitted 14 March 2020, Revised 12 April 2020, Accepted 03 May 2020.

Abstract: Polypropolyene (PP) is commonly used in geotextile mat reinforcements for landfill systems due to its unique properties which must be carefully selected to ensure adequate performance of the PP material. To achieve this, supplier information for the PP material which included tensile strength, mass and thickness were simulated as input variables for twelve scenarios each using SOLIDWORKS and Response Surface Methodology (RSM) software. The goal was to minimize stress, resultant displacement and equivalent strain to avoid the catastrophic effect that may occur when the goal is opposite. In comparison to other scenarios, RSM in the 4th scenario probed the input values by indicating that input values of 1.5 mm thickness, 3110.54 g of mass and tensile strength of 33 MPa produced optimum output values of 27418 N/m^2 stress, 0.000102754 mm displacement and 0.000007452 strain. Similarly in the 7th scenario, SOLIDWORKS probed the input values by indicating that input values of 1.6 mm thickness, 3110.54 g of mass and tensile strength of 33 MPa produced optimum output values of 26984 N/m^2 stress, 0.000102614 mm displacement and 0.000007152 strain. The proximity observed in the selected results generated by both software indicates a level of accuracy that can sustain the service life of the PP material in landfill applications if adopted by manufacturers.

Keywords: Clogging; Geotextile mat; Landfill; Leachate; Modelling; Polypropylene; Sold waste.

1. INTRODUCTION

The leachate collection system of a typical landfill system consists of moderately permeable drainage layer, perforated pipes, leachate collection sump, and geotextile mat which protects the landfill bottom liner from damages or clogging of the drainage layer [1, 2]. Carey *et al*. [3] described clogging as the accumulation of debris, sand, silt particles, tiny organic or inorganic materials in the landfill drainage pipes, drainage or filter layers, thereby, preventing leachate from flowing freely across the landfill layers as well as the drainage pipes. This usually cause difficulties during the process of extracting leachate from the landfill systems.

Typical drainage layer in a landfill system consists of a high-porosity medium that provides variable flow paths into the perforated leachate collection pipes and the collection sump [4]. In order to prevent capillary action and clogging from retaining leachate in the drainage layer, coarse material is applied to provide sufficient space within the drainage layer to enable leachate drain freely [5]. This creates room for leachate to flow within the drainage media, thereby, reducing the possibility of clogging [3, 6]. Installation of geotextile mat is usually between the waste layers and the drainage materials which reduces the ingress of small grained particles into the gravel layer (drainage layer) in order to prevent clogging of any section in the landfill system [7]. In other words, the geotextile mat also known as geotextile filters allows the free flow of landfill leachate while retaining solid particles that may hamper its movement.

Apart from landfill leachate collection system, geotextile filters also play a significant role in French drains, highway edge drains, retaining wall drainage systems etc. Geotextile mat is manufactured mostly from a combination of polypropylene (PP) which is a thermoplastic resin made by the polymerization of propylene and other materials to form composite material but this framework is based on the service life of polypropylene material [8]. However, there is currently no method to determine the service life of this drainage media or the rate at which clogging occurs around the geotextile material. This is due to reduction in porosity and hydraulic conductivity which indicates failure of geotextile media or drainage layer as a result of biological and chemical activities of microorganisms in landfill systems [9]. A simple model that can be employed by practitioners to estimate the service life of numerous drainage designs was developed based on the findings from laboratory

(mesocosm) and field exhumation studies [10]. Such laboratory test for example, may also include the standard (ASTM D-5567-11) test method for Hydraulic Conductivity Ratio (HCR) for geotextile systems, and standard (ASTM D-4751-12) test method for determining Apparent Open Size (AOS) of a geotextile material among others [11, 12].

Kada *et al*. [13] investigated the physical and mechanical properties of polypropylene-wood-carbon fibre hybrid composites and found out that hybridization can improve the strength and tensile properties of PP. Al-Shabanat [14] investigated the degradation behavior of PP material under natural weather condition (29-35^{o} C) in Saudi Arabia and found out that the mechanical properties decreased after exposure period of six months due to the effect of polymer degradation as a result of natural photo-oxidation of the PP material.

The service condition of a polypropylene geotextile materials and its composites depend on organic loading acting statically on each point of installation, during which the material is subjected to physical forces and it undergoes displacements in addition to the biological and chemical reactions that will occur in the landfill surroundings. The service life of this material may also depends on the type of waste material and age of the landfill system. For example, some waste materials contain compounds such as ammonium, heavy metals, chlorinated organic compounds, benzene, toluene and xylenes among others which can potentially hamper the mechanical properties and performance of this material [15, 16]. This agrees with the findings of [17], that acidic/alkaline leachate as well as metallic ions (particularly cupric ions) in Municipal Solid Waste (MSW) and long term ultraviolet radiation can influence the mechanical properties of geotextile material.

Geomembranes are typically used as hydraulic barriers while geotextiles protect it from in-service damages such as high normal stresses and angular soil particles [18, 19]. Geotextiles are geosynthetic fabrics that are fabricated to be porous, flexible and permeable, and can be classified either as woven or nonwoven with respect to the method in which they are manufactured [20]. Geotextiles are commonly produced from polypropylene or polyester and fabricated into the following categories of fabric: woven slit-film monofilament, woven multifilament, woven slit-film multifilament, woven monofilament, nonwoven continuous filament heat bonded, nonwoven continuous filament needle-punched, nonwoven resin bonded, and nonwoven staple needle-punched [21].

According to [22], woven geotextiles serve as reinforced materials that provide sufficient tensile strength to landfill drainage media with low tensile capacity, whereas, the nonwoven geotextiles allow the flow of liquid or gas across the landfill layers while retaining solid particles within the flow stream. The properties of a geotextile mat can be classified as: Physical properties (stiffness, density, specific gravity, weight and thickness), mechanical properties (tensile strength, tenacity, drapability, friction resistance, static puncture resistance, elongation, abrasion resistance, flexibility and tearing strength), hydraulic properties (porosity, turbidity, transitivity, permeability, permittivity and filtration length) and degradation properties (hydraulic degradation, chemical degradation, biodegradation, photo degradation and mechanical degradation) [23, 24].

Bacasm et al. [25] studied the shear interaction mechanism of one of the critical interfaces in geotextiles typically used in landfills. The test results revealed a strain softening behavior with very small dilatancy (< 0.5 mm) and nonlinear failure enveloped at a normal stress range of 25-450 kPa. From the three geotextiles tested, the thermally bonded monofilament exhibited the best interface shear strength under high normal stress. For low normal stress, needle-punched monofilaments were recommended. For the regular textured geomembranes, the space between the asperities played an important role while the nonwoven geotextiles made of monofilaments produce the largest interface shear strength for the irregular textured geomembranes.

ASTM D5101 test method was used to evaluate the index properties and clogging performance of combining a hybrid geotextile with the conventional drainage composite. The result revealed that a double layered geotextile material combining nonwoven and woven geotextiles into one needle punched hybrid geotextile offers improved tensile strength, resistance to induced stress failure as well as effective separation and drainage in landfill applications. The case study was presented for the protective cover and drainage composite layers in fly ash landfill expansion [26, 27]. Zhao and Karim [28] recommended factor of safety of 1.5 and above for the design of landfill materials like the geotextile mat which is subjected to static loads during service condition.

This study is focused on the selection of optimum properties for polypropylene material suitable for landfill basal geotextile application. This was achieved using computer aided tools to simulate the input variables (which were the parameters obtained from the geotextile mat supplier) extrapolated at different scenarios to obtain output responses among which the optimum parameters were selected.

2. MATERIALS AND METHODS

PP of 18.5x18.5 m was purchased from the open market for the purpose of constructing a landfill prototype for organic waste management and energy generation in terms of landfill gas. The descriptions of the PP material provided during purchase were melting point temperature (30^{o} C), range of tensile strength between 31.03-41.37 MPa (ISO527), mass (9613.75 g) and thickness (4.5 mm). This information were applied as input variables in order to establish the output requirement such as stress, equivalent strain and resultant displacement. The geotextile mat was modelled using Response Surface Methodology (RSM) and SOLIDWORKS with polypropylene selected for the model as shown in Figure 1. The model type was linear elastic isotropic and was subjected to static analysis with a load condition of 1000 kg considered as the total mass of organic waste to be deposited in the landfill system. To obtain optimal output solution of the analysis, 12 simulated scenarios were generated using RSM and SOLIDWORKS on the basis of the following input constraints: optimum thickness, optimum mass, maximum tensile strength and output constraints; minimum stress, minimum strain and minimum displacement. Results obtained as optimum scenario from RSM and SOLIDWORKS were used as specification in the open market to purchase polypropylene material which was subjected to tensile test according to ISO527 standard. Using equation 1, the yield strength was calculated by dividing the load at breakage by the minimum cross sectional area of the PP.

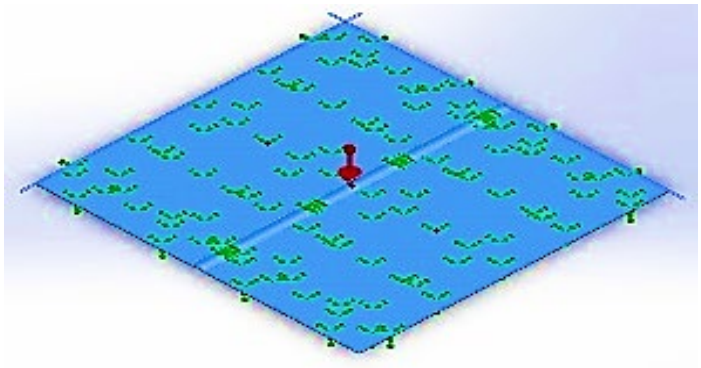

Figure 1. Polypropylene-based geotextile model using SOLIDWORKS

$$\text{Tensile Strength} = \frac{\text{Load at breakage}}{\text{Original length} \times \text{Original thickness}} \quad (1)$$

$$\text{Experimental tensile strength} = \frac{1000}{18.5 \times 1.5} = 36 \text{ MPa}$$

In this study, statistical design of experiment (DOE) was carried out using the central composite design method (CCD) which is an acceptable design approach for RSM. The design and optimization was carried out using Design Expert 7.01 as the design software. Based on the DOE, an experimental design matrix having six centre points, six axial points and eight factorial points resulting in twenty experimental runs was generated. The twenty experimental runs were exported to SOLIDWORKS software, where design study was conducted based on the input variables (thickness: 4.5 mm, mass: 9613.75 g, tensile strength: 31.03 MPa) and twelve optimum scenarios were selected for detailed analysis. The twelve optimum scenarios were based on the constraint specified for each parameter shown in Table 1. The randomized design matrix comprised of three input variables, namely: thickness (mm), mass (g), tensile strength (MPa) as well as three response variables, namely: stress (N/m^2), displacement (mm) and strain.

The sequential model sum of squares indicated the accumulating improvement in the model fit as terms are added. Based on the calculated sequential model sum of square, the highest order polynomial where the additional terms are significant and the model is not aliased was selected as the best fit. It was observed that the cubic polynomial was aliased hence cannot be employed to fit the final model. In addition, the quadratic and 2FI model were suggested as the best fit thus justifying the use of quadratic polynomial in this analysis. To test how well the quadratic model can explain the underlying variation associated with the experimental data, the lack of fit test was estimated for each response. While a model with significant lack of fit cannot be employed for prediction, non-significant lack of fit is good, as it indicates a model that is significant. The model summary statistics of model fit shows the standard deviation (Root Mean Square Error-RMSE), the r-squared and adjusted r-squared, predicted r-squared and the PRESS statistic for each complete model. Low standard deviation, R-Squared near 1 and relatively low PRESS are the optimum criteria for defining the best model source.

Based on the simulation outcome, the quadratic polynomial model was suggested while the cubic polynomial model was aliased, thus, the quadratic polynomial model was selected for this analysis. Analysis of the model standard error was employed to assess the suitability of response surface methodology using the quadratic model to minimize stress, minimize displacement and minimize the strain on the geotextile mat. Analysis of variance (ANOVA) was used to check whether or not the model is significant and also to evaluate the significant contributions of each individual variable, the combined and quadratic effects towards each response. To validate the adequacy of the quadratic model based on its ability to minimize stress, minimize displacement and minimize the strain, goodness of fit statistics were employed. To obtain the optimal solution, the coefficient statistics and the corresponding standard errors were first considered. The computed standard error measures the difference between the experimental terms and the corresponding predicted terms.

3. RESULTS AND DISCUSSION

From the Analysis of variance (see Table 1) for response surface quadratic model in validating the model significance towards minimizing induced stress on the geotextile mat, the Model F-value of 53.12 implies that the model is significant. There is only a 0.01% chance that a "Model F-Value" this large could occur due to noise. Values of "Prob > F" (P-value) less than 0.0500 indicate model terms are significant. Values greater than 0.1000 indicate the model terms are not significant. From the analysis of variance in this study, the "Lack of Fit F-value" of 0.45 indicates that the Lack of Fit is not significant relative to the pure error. There is a 79.38% chance that a "Lack of Fit F-value" this large could occur due to noise. Non-significant lack of fit is good as it indicates a model that is significant.

From the Analysis of variance (see Table 1) for response surface quadratic model in validating the model significance towards minimizing Resultant displacement on the geotextile mat, the Model F-value of 26.24 implies that the model is significant. There is only a 0.01% chance that a "Model F-Value" this large could occur due to noise. Values of "Prob > F" (P-value) less than 0.0500 indicate that model terms are significant. Values greater than 0.1000 indicate the model terms are not

significant. From the analysis of variance in this study, the "Lack of Fit F-value" of 0.82 indicates that the Lack of Fit is not significant relative to the pure error. There is a 57.70% chance that a "Lack of Fit F-value" this large could occur due to noise. Non-significant lack of fit is good as it indicates a model that is significant.

For response surface quadratic model in validating the model significance towards minimizing equivalent strain on the geotextile mat, the Model F-value of 24.50 implies that the model is significant. There is only a 0.01% chance that a "Model F-Value" this large could occur due to noise. Values of "Prob > F" (P-value) less than 0.0500 indicate model terms are significant. Values greater than 0.1000 indicate the model terms are not significant. From the analysis of variance in this study, the "Lack of Fit F-value" of 3.10 indicates that the Lack of Fit is not significant relative to the pure error. There is a 11.65% chance that a "Lack of Fit F-value" this large could occur due to noise. Non-significant lack of fit is good as it indicates a model that is significant.

As shown in Table 2, the design study indicated that scenario 4 met the design constrain specified for the analysis. To study the effects of combine variables on each response; the following 3D surface plots presented in Figures 2-4 were employed.

Table 1. ANOVA table for validating the model significance

Induced Stress					
Source	Sum of squares	df	Mean square	F value	P-value (Prob>F)
Model	21.26	9	2.32	53.12	<0.0001
Lack of Fit	0.14	5	0.028	0.45	0.7938
Resultant Displacement					
Source	Sum of squares	df	Mean square	F value	P-value (Prob>F)
Model	47196.69	9	5244.08	26.24	<0.0001
Lack of Fit	904.26	5	180.85	0.82	0.5760
Equivalent Strain					
Source	Sum of squares	df	Mean square	F value	P-value (Prob>F)
Model	57617.27	9	6401.92	24.50	<0.0001
Lack of Fit	1897.73	5	379	3.10	0.1165

Table 2. Predicted input variables and output responses for different scenarios in RSM

Parameters	Units	Input (Supplier details)	Output (Simulated)	Constraints	Scenario 1	Scenario 2
Thickness	mm	4.5	-	Optimum	1.5	3
Mass	g	9613.75	-	Optimum	3157.06	6314.13
Tensile Strength	MPa	-	34.2	Maximum	27.13	29.32
Stress	N/m^2	-	29742	Minimum	28901	29673
Displacement	mm	-	0.004629351	Minimum	0.004360182	0.006340178
Strain	mm	-	0.000246457	Minimum	0.000347421	0.0005158841
Parameters	Units	Scenario 3	Scenario 4	Scenario 5	Scenario 6	Scenario 7
Thickness	mm	4.5	1.5	3	4.5	1.5
Mass	g	9471.2	3110.54	6473.88	9712.22	3207.57
Tensile strength	MPa	26.23	33.00	27.13	26.26	29.12
Stress	N/m^2	27681	27418	28853	30100	29142
Displacement	mm	0.004834017	0.000102754	0.007380143	0.009250735	0.003642853
Strain	-	0.004123857	0.000007452	0.004126852	0.000096854	0.002826419
Parameters	Units	Scenario 8	Scenario 9	Scenario 10	Scenario 11	Scenario 12
Thickness	mm	3	4.5	1.5	3	4.5
Mass	g	6415.19	9622.87	3204.57	6409.15	9613.75
Tensile strength	MPa	28.16	30.24	26.17	27.27	29.35
Stress2	N/m^2 (MPa)	30132	29764	28967	28652	29753
Displacement	mm	0.065120157	0.007231367	0.0028543574	0.004215746	0.008620154
Strain	-	0.003826296	0.000846732	0.0007626643	0.004146752	0.000436764

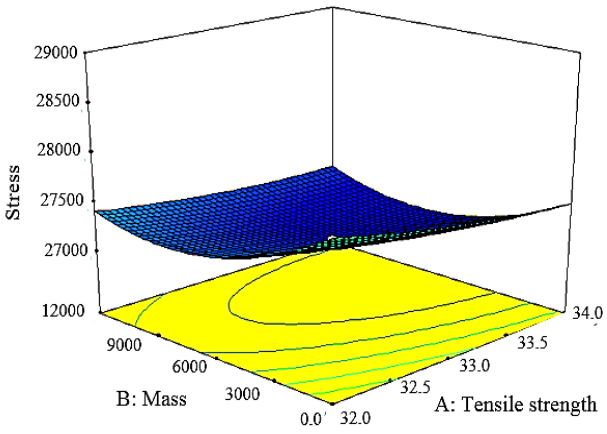

Figure 2. Effect of mass and tensile strength on stress properties of polypropylene

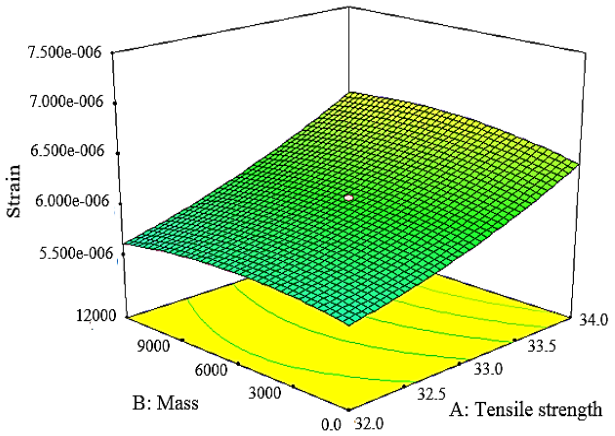

Figure 3. Effect of mass and tensile strength on strain properties of polypropylene

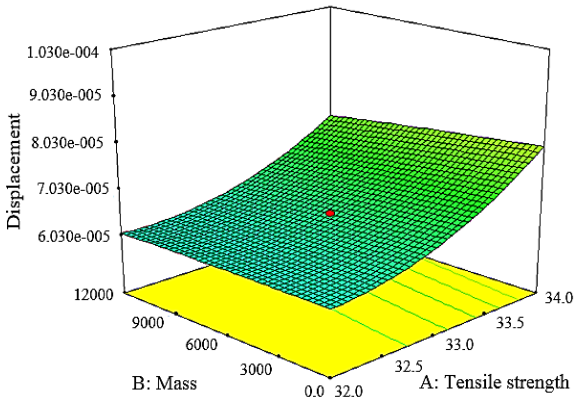

Figure 4. Effect of mass and tensile strength on displacement of polypropylene

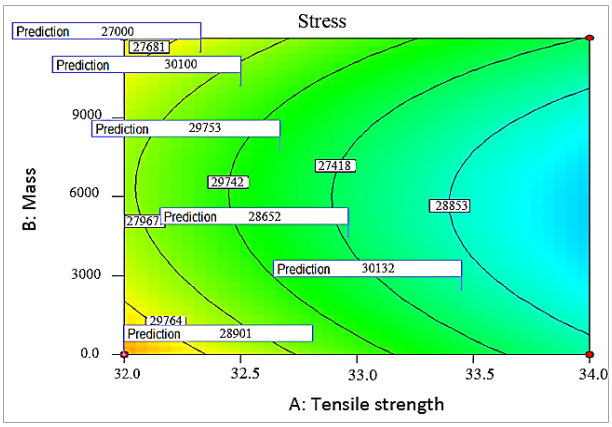

Figure 5. Predicting the stress using contour plot

Figure 2 shows a 3 dimensional contour plot which was employed to give a clearer concept of the response surface and the relationship between the variables on the response. As the color of the curved surface gets darker, the stress distribution gets higher while the strain and displacement increases proportionately. The presence of a colored hole at the middle of the upper surface gave a clue that more points lightly shaded for easier identification fell below the surface. To study the effects of combine variables on each response; equivalent strain 3D surface plot presented in Figure 3 was employed. Three dimensional surface plots was employed to give a clearer concept of the surface response. The presence of a colored hole at the middle of the upper surface gave a clue that more points lightly shaded for easier identification fell below the surface. To study the effects of combine variables on each response, 3D surface plot was employed for the resultant displacement as presented in Figure 4. The 3D surface plots as observed in Figures 2-4 indicates the relationship between the input variables (thickness, mass and tensile strength) and the output responses (stress, strain and displacement).

Numerical optimization was performed to ascertain the desirability of the overall model. In the numerical optimization phase, design expert was programed to minimize the stress while also determining the optimum value of thickness, mass and tensile strength. Based on the optimal solution, the contour plots showing the stress output responses against the optimized values of the input variable are presented in Figure 5.

The contour plots in Figure 5 indicate different predictions such as tensile strength of 32.0, 32.5 MPa, 33.0 MPa and 33.5 MPa, stresses of 27967 MPa, 28901 MPa, 27418 MPa and 28853 MPa. Based on the optimal solution, the contour plots showing the strain response variable against the optimized value of the input variable is presented in Figure 6. The contour plots in Figure 6 show different predictions such as tensile strength of 32.0 MPa, 32.5 MPa, 33.0 MPa and 33.5 MPa, strain of 0.000096854, 0.000246457, 0.000007452 and 0.002826419. From the optimal solution, the contour plots showing the displacement output response against the optimized value of the input variable is presented in Figure 7. The contour plots in Figure 7 represent different predictions such as tensile strength of 32.0 MPa, 32.5 MPa, 33.0 MPa and 33.5 MPa, displacements of 0.009250735 mm, 0.004215746 mm, 0.000102754 mm and 0.0028543574 mm.

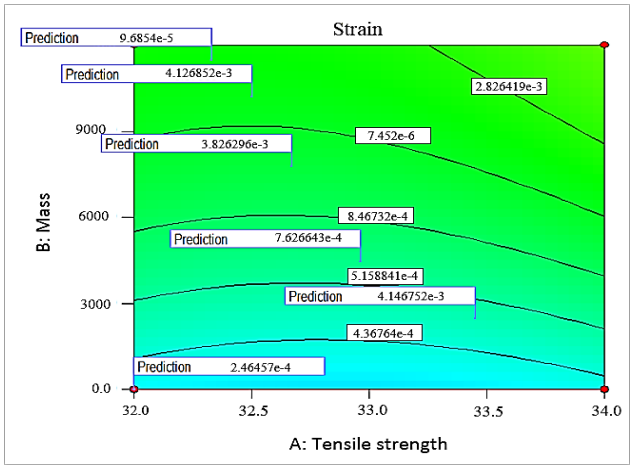

Figure 6. Predicting the strain using contour plot

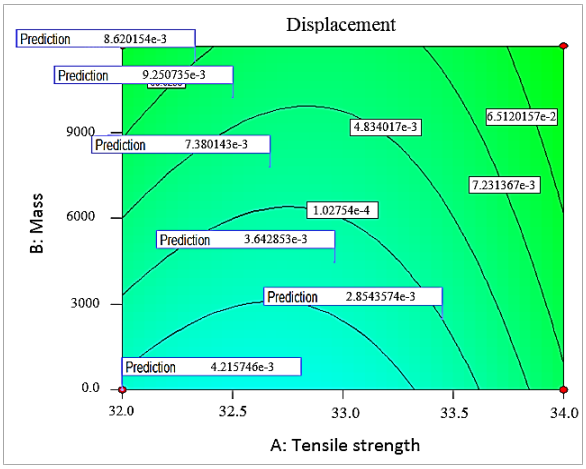

Figure 7. Predicting the displacement response using contour plot

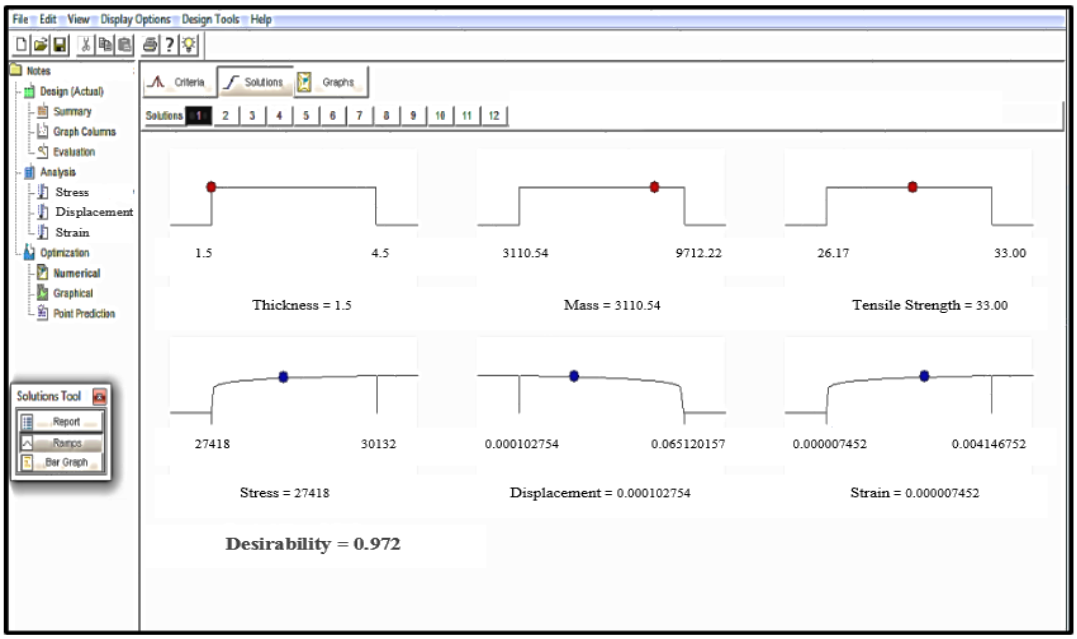

Figure 8. Ramp solution of numerical optimization

From the results presented in Table 2, scenario 4, it can be observed that geotextile mat thickness of 1.5 mm, mass of 3110.54 g and tensile strength of 33.00 MPa will produce the following optimum responses suitable for landfill application:

a) Induced stress distribution: 27418 N/m^2
b) Resultant displacement: 0.000102754 mm
c) Equivalent strain: 0.000007452

This solution was selected by design expert as the optimal solution with a desirability value of 97.20%. The ramp solution is the graphical presentation of the optimal solution as shown in Figure 8, while the desirability bar graph which shows the accuracy with which the model is able to predict the values of the selected input variables and the corresponding responses [29] is presented in Figure 9. It can be deduced from the result of Figure 9 that the model developed based on response surface methodology and optimized using numerical optimization method, predicted the following responses:

a) Induce stress with an accuracy level of 95.06%
b) Resultant displacement with an accuracy level of 98.73%
c) Equivalent strain with an accuracy level of 97.86%

The predicted input variables and output responses for different scenarios in SOLIDWORKS are presented in Table 3. Optimal values for the predicted tensile strength and experimental tensile strength are shown in Figure 10. For the predicted values, optimal solution was found in scenario 4 of Table 2 using RSM while optimal solutions was found in scenario 7 of Table 3 using SOLIDWORKS. Figure 11-13 represents SOLIDWORKS parametric distribution profile of optimum values for stress, strain and displacement.

Figure 9. Prediction accuracy of numerical optimization

Table 3. Predicted input variables and output responses for different scenarios using SOLIDWORKS

Parameters	Units	Input (Supplier details)	Output (Simulated)	Constraints	Scenario 1	Scenario 2
Thickness	mm	4.5	-	Optimum	1.5	3
Mass1	g	9613.75	-	Optimum	3111.19	6222.4
Tensile strength	MPa	31.03	34.0	Maximum	27.10	27.06
Stress2	N/m^2	-	29634	Minimum	28432	29811
Displacement	mm	-	0.003565641	Minimum	0.02465630	0.004869442
Strain	-	-	0.000247354	Minimum	0.006286331	0.004392841
Parameters	Units	Scenario 3	Scenario 4	Scenario 5	Scenario 6	Scenario 7
Thickness	mm	4.5	1.5	3	4.5	1.5
Mass1	g	9333.63	3110.64	6221.29	9331.93	2930.81
Tensile strength	MPa	28.60	26.12	29.07	28.03	32.80
Stress2	N/m^2	28213	27984	27953	28126	26984
Displacement	mm	0.000463123	0.005721349	0.004238347	0.006251854	0.000102614
Strain	-	0.000679533	0.000073827	0.006573627	0.0005954341	0.000007152
Parameters	Units	Scenario 8	Scenario 9	Scenario 10	Scenario 11	Scenario 12
Thickness	mm	3	4.5	1.5	3	4.5
Mass1	g	6221.09	9331.64	3163.17	6326.5	9489.98
Tensile strength	MPa	27.14	26.23	30.16	29.02	27.17
Stress2	N/m^2	29764	29547	28112	27841	29653
Displacement	mm	0.004537812	0.000502492	0.003849375	0.005320186	0.000743827
Strain	-	0.0003748519	0.0006258841	0.002419836	0.008231863	0.007126848

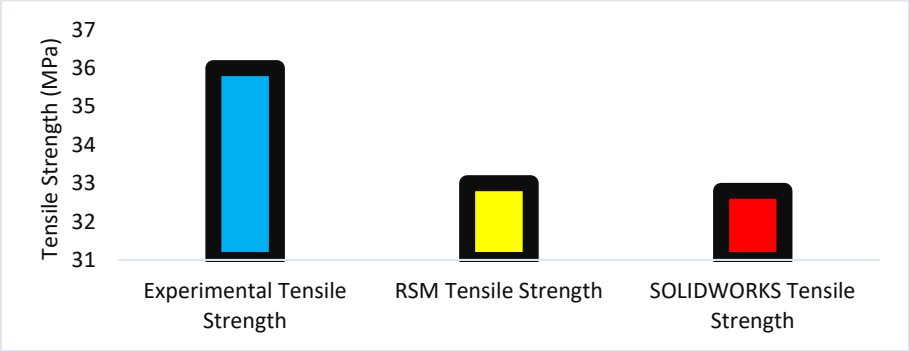

Figure 10. Experimental and predicted tensile strength

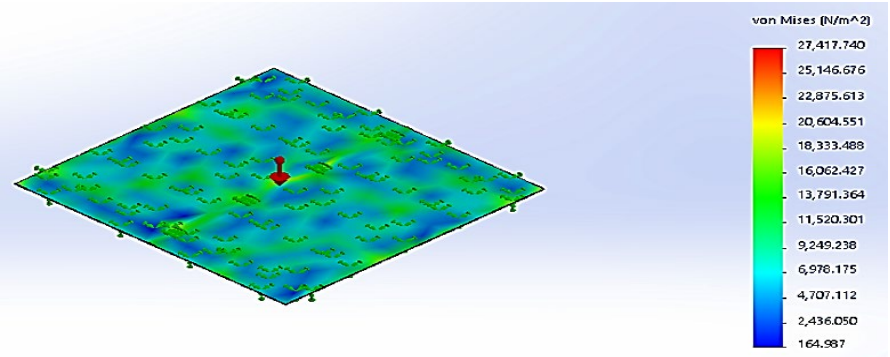

Figure 11. Static stress distribution on the polypropylene-based geotextile

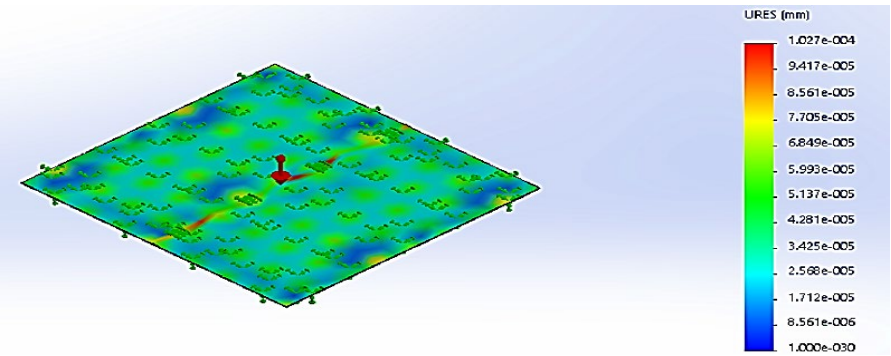

Figure 12. Resultant displacement on the polypropylene-based geotextile

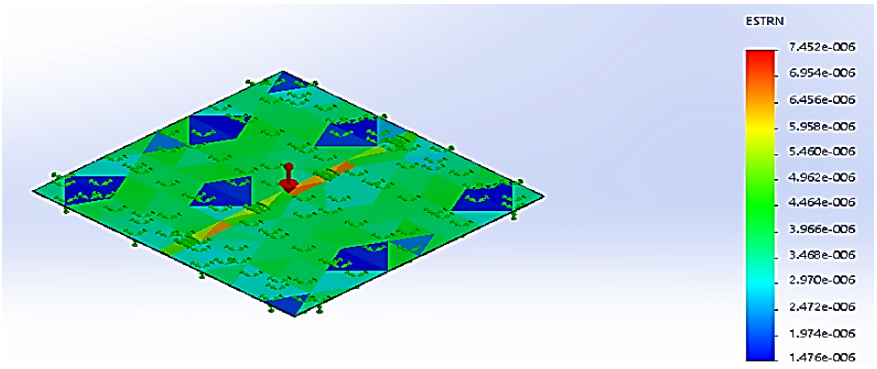

Figure 13. Equivalent strain on the polypropylene-based geotextile

From Figure 10, RSM-predicted value for tensile strength (33 MPa) is much closer to the tensile strength value predicted by SOLIDWORKS (32.8 MPa) unlike the tensile strength value (36 MPa) calculated from the experimental data. The

difference between the experimental tensile strength value and RSM-predicted tensile strength value is 3MPa, while the difference between experimental tensile strength value and the SOLIDWORKS-predicted tensile strength value is 3.2MPa. The effect of the aforementioned difference to the performance of the geotextile mat is not considered to be significant, because the experimental and predicted tensile strength values are higher than the manufacturer or supplier tensile strength value (31.03 MPa). This implies that the geotextile mat which is practically under tension (as it is laid between the landfill subgrade and the compacted waste stream) in its service condition will exhibit higher resistance against the tensile forces acting on it or possess huge capacity to accommodate tensile stresses while it stretches or pulls before tearing. The large difference between the experimental values and the predicted values could be as a result of errors during the experiment. Possible sources of error in this case are highlighted as follows [30]:

a) Linearity: pressure changes may affect the sensitivity of the gauge, especially when the capacity of the gauge is exceeded.
b) Hysteresis: this means the gauge does not return to zero after load is withdrawn.
c) External errors: due to overloading, wind loading, shock loading, vibration, temperature changes or movement of the loading frame as well as the weighing equipment.

From the static simulation results in Figure 11, the maximum stress induced in the geotextile mat is 27417.7 N/m^2, which is well below the yield strength of the material (34000000 N/m^2), indicating that the geotextile mat will not fail with the present load conditions (1000 kg).This relates to von-Mises yield criterion also known as maximum distortion criterion. This is governed by plasticity theory which states that yielding begin in ductile materials when the second invariant of deviatoric stress attains a critical value [31, 32]. It can also be used in the prediction of yielding in a given material subjected to variable loads. According to Ikpe *et al.* [33], any given material under such loading condition may be considered to have started yielding when its maximum von-Mises stress is close to or reaches the yield strength of the material and considered to have failed when the von-Mises stress exceeds the material yield strength. In other words, if the von-mises stress value is much less than the material's yield strength, it can be considered that the material still has the capacity to accommodate further forces/loads before failure [34].

The corresponding maximum displacement is 0.000102736 mm as shown in Figure 12, while the maximum strain is 0.000007452 as shown in Figure 13. Design study was carried out for twelve (12) scenarios to determine the optimal geotextile thickness, mass and maximum tensile strength as well as minimum stress, minimum resultant displacement and minimum equivalent strain for optimum service life of the material. As shown in Table 3, the design study indicated that scenario 7 met the design constraint specified for the analysis.

4. CONCLUSION

The predicted optimum values for mass of the polypropylene material were lower than the specified mass in the supplier catalogue. The significance is that the load burden per unit area constituted by lightweight materials on the drainage layer of a landfill system would be less and vice versa. This will sustain the structural integrity of the system despite the harsh condition it undergoes. Similarly, the predicted optimum values for the thickness of polypropylene material were lower than the original thickness specified mass in the supplier's catalogue. The significance is that lower thickness of geotextile (which is primarily made of polypropylene) reduces the possibility of clogging. Finally, the predicted optimum values for tensile strength were higher than the ones specified in the supplier catalogue. This indicates that the higher the tensile strength of the material, the less prone the material is to tensile failure due to organic loading. Simulation of the three input variables (thickness of 4.5 mm, mass of 9613.75 g and tensile strength of 31.03 MPa) obtained from the geotextile mat supplier generated optimum responses (RSM responses: thickness of 1.5 mm, mass of 3110.54 g and tensile strength of 33 MPa; SOLIDWORKS responses: thickness of 1.5 mm, mass of 2930.81 g and tensile strength of 32.80 MPa) that resulted in minimum stress, strain and displacement response of the geotextile mat. This therefore indicates that with minimum stress level, minimum equivalent strain and minimum resultant displacement; the polypropylene material can meet its service life if the constituting input are selected properly. This was further proven in SOLIDWORKS static analysis where the von-mises stress was below the yield strength of the polypropylene material. Also, there was close correlation in the values generated from the two software, indicating that computer aided tools can be employed in addition to experimental analysis to determine optimal parameters before manufacturing.

REFERENCES

[1] EPA Environmental Protection Agency, *Siting, Design, Operation and Rehabilitation of Landfills. Best Practice Environmental Management*. Carlton: 2014.

[2] A. E. Ikpe, A. E. Nndon and A. U. Adoh, Modelling and simulation of high density polyethylene liner installation in engineered landfill for optimum performance, *Journal of Applied Science and Environmental Management,* 23(3), 2019, 449-456.

[3] P. Carey, G. Carty, B. Donlon, D. Howley and T. Nealon, *Landfill Manuals Landfill Site Design*. Environmental Protection Agency, Ireland: 2000.

[4] G. Lee, L. Anne and L. Fred, *Overview of Subtitle D Landfill Design, Operation, Closure and Postclosure Care Relative to Providing Public Health and Environmental Protection for as Long as the Wastes in the Landfill will be a Threat*. El Macero, Canada: 2004.

[5] S. Yedla, Modified landfill design for sustainable waste management, *International Journal of Global Energy Issues,* 23(1), 2005, 93-105.
[6] H. Ramke, Leachate collection systems, *Proceedings of the 1st Middle European Conference on Landfill Technology*, Budapest, Hungary, 2008.
[7] N. E. Shahabi, S. Saharkhiz, M. H. Varkiyani and S. Mohammad, Effect of fabric structure and weft density on the poisson's ratio of worsted fabric, *Journal of Engineered Fibres and Fabrics,* 8(2), 2013, 63-17.
[8] B. J. Agrawal, Geotextile: It's application to civil engineering – Overview, *National Conference on Recent Trends in Engineering and Technology,* India, 2011, 1-6,
[9] R. K. Rowe and J. F. VanGulck, Filtering and drainage of contaminated water, *4th International Conference on Geofilters*, Stellenbosch, South Africa, 2004, 1-63.
[10] R. K. Rowe and I. R. Fleming, Estimating the time for clogging of leachate collection systems, *Proceedings of 3rd International Congress on Environmental Geotechnics*, Lisbon, Portugal, 1998, 23-28.
[11] ASTM American Society for Testing and Materials, *ASTM D-5567-11 Standard Test Method for Hydraulic Conductivity Ratio (HCR) Testing of Soil/Geotextile Systems*, West Conshohocken, PA: 2011.
[12] ASTM American Society for Testing and Materials, *ASTM D-4751-12 Standard Test Method for Determining Apparent Open Size of a Geotextile*. West Conshohocken, PA: 2012.
[13] D. Kada, S. Migneault, G. Tabak and A. Koubaa, Physical and mechanical properties of polypropylene-wood-carbon fiber hybrid composites, *Bioresources,* 11(1), 2016, 1393-1406.
[14] M. Al-Shabanat, Study of the effect of weathering in natural environment on polypropylene and its composites: morphological and mechanical properties, *International Journal of Chemistry,* 3(1), 2011, 129-141.
[15] A. F. Al-Yaqout and M. F. Hamoda, Evaluation of landfill leachate in arid climate-A case study, *Environment International,* 29(5), 2003, 593-600.
[16] K. Y. Foo, L. K. Lee and B. H. Hameed, Batch adsorption of semi-aerobic landfill leachate by granular activated carbon prepared by microwave heating, *Chemical Engineering Journal,* 222, 2013, 259-264.
[17] X. Long, L. He, Y. Zhang and M. Ge, Multicomponent composite emulsion treated geotextile on landfill with improved long-term stability and security, *Journal of Engineering Fibres and Fabrics,* 13(3), 2018, 59-70.
[18] G. L. Hebeler, J. D. Frost and A. T. Myers, Quantifying hook and loop interaction in textured geomembrane-geotextile systems, *Geotextiles and Geomembranes,* 23(1), 2005, 77-105.
[19] H. N. Pitanga, J. P. Gourc and O. M. Vilar, Interface shear strength of geosynthetics: evaluation and analysis of inclined plane tests, *Geotextiles and Geomembranes,* 27(6), 2009, 435-446.
[20] S. C. Das, D. Paul, M. M. Fahad, T. Islam and E. H. Nizam, Geotextile-A potential technical product, *Journal of Scientific and Engineering Research,* 4(10), 2017, 337-350.
[21] M. Ashis, Application of geotextiles in coastal protection and coastal engineering works: An overview, *International Research Journal of Environment Sciences,* 4(4), 2015, 96-103.
[22] A. Bouazza, J. G. Zornberg and D. Adam, Geosynthetics in waste containment facilities: Recent advances, *Geosynthetics,* 2, 2002, 445-510.
[23] B. J. Agrawal, Geotextile: Its application to civil engineering – Overview, *National Conference on Recent Trends in Engineering and Technology,* Gujarat, India, 2011.
[24] U. P. Kelechi and O. C. Okeke, Geotextile and geomembrane: Properties, production and engineering applications, *International Journal of Advanced Academic Research,* 4(11), 2018, 17-32.
[25] B. M. Bacasm, J. Cañizal and H. Konietzky, Shear strength behaviour of geotextile/geomembrane interfaces, *Journal of Rock Mechanics and Geotechnical Engineering,* 7, 2015, 638-645.
[26] M. Kutay and A. Aydilek, Filtration performance of two-layer geotextile systems, *Geotechnical Testing Journal,* 28(1), 2012, 79-91.
[27] G. Ahlberg, W. Lupi, N. Parks, N. Patel and A. Shah, Hybrid geotextile design for ccr materials in landfill drainage and closure systems, *World of Coal Ash (WOCA) Conference,* Nasvhille, 2015, 1-12.
[28] L. Zhao and M. A. Karim, Use of geosynthetic materials in solid waste landfill design: A review of geosynthetic related stability issues, *Annals of Civil Environmental Engineering,* 2, 2018, 6-15.
[29] A. E. Ikpe and I. Owunna, Optimization of TIG welding input variables for AISI 1020 low carbon steel plate using response surface methodology, *International Journal of Engineering Science and Application,* 2(3), 2018, 114-122.
[30] A. E. Ikpe, I. Owunna and P. O. Ebunilo, Determining the accuracy of finite element analysis when compared to experimental approach for measuring stress and strain on a connecting rod subjected to variable loads, *Journal of Robotics, Computer Vision and Graphics,* 1(1), 2016, 12-20.
[31] A. E. Ikpe, I. B. Owunna and P. Satope, Design optimization of a B-pillar for crashworthiness of vehicle side impact, *Journal of Mechanical Engineering and Sciences*, 11(2), 2017, 2693-2710.
[32] I. B. Owunna and A. E. Ikpe, Evaluation of induced residual stresses on AISI 1020 low carbon steel plate from experimental and FEM approach during TIG welding process, *Journal of Mechanical Engineering and Sciences,* 13(1), 2019, 4415-4433.
[33] A. E. Ikpe, O. E. Efe-Ononeme and G. O. Ariavie, Thermo-structural analysis of first stage gas turbine rotor blade materials for optimum service performance, *International Journal of Engineering and Applied Sciences,* 10(2), 2018, 118-130.
[34] A. E. Ikpe and I. Owunna, Design of vehicle compression springs for optimum performance in their service condition, *International Journal of Engineering Research in Africa,* 33, 2017, 22-34.